Criticality of forcing directions on the fragmentation and resilience of grid networks

Cheryl Abundo, Christopher Monterola, Erika Fille Legara

CONTENTS

S1. NETWORK ELONGATION

Initially, each edge is assigned an elongation threshold ε_{th}. Before the crack propagation begins, the edges are structurally reinforced randomly such that the elongation thresholds of the edges are between 0.0500 and 0.0550, similar to the method employed in fracture propagation [1]. Every two connected nodes differ in the amount of force loading they can manage to have between them. Randomly assigning elongation threshold values takes into account this disparity.

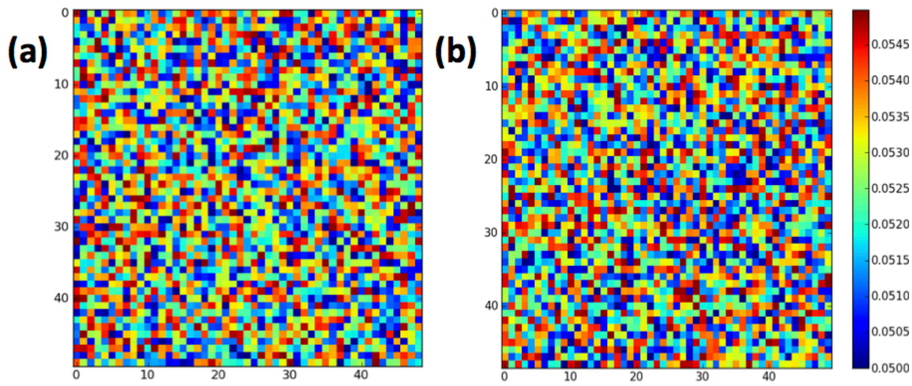

FIG. S1: *Random reinforcement of network edges.* (a) Elongation thresholds of the horizontal edges and (b) elongation thresholds of the vertical edges in the lattice network.

The displacement of each node of mass m is then computed according to the breaking dynamics of the configuration in Fig. S2. If the displacement of a particular node causes one of its edges to elongate beyond its threshold then the link is considered broken and removed from succeeding iterations of the simulation.

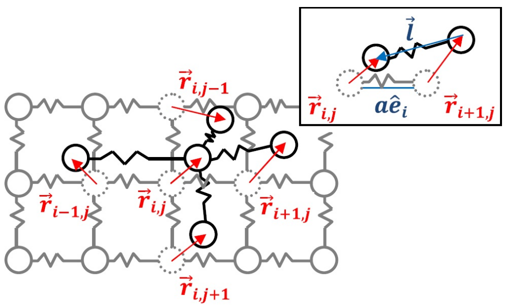

FIG. S2: *Body diagram.* Displacement of the $(i, j)^{th}$ node and its four nearest neighbors.

S2. NUMERICAL STABILITY

The $2N^2$ equations for node positions and $2N^2$ equations for velocities were solved using the fourth order Runge-Kutta (RK4) method with known local discretisation error $O(\delta t^5)$ per time step iteration [1]. For $\delta t = 2^{-10}$, the local error $\delta\xi_L$ is negligible at $9x10^{-16}$ per RK4 application. The global error $\delta\xi$, on the other hand, is $O(\delta t^4)$ and for our simulations involving an NxN grid network described by $4N^2$ differential equations, the total accumulated error for the entire network lifetime t_f is $\delta\xi \sim 4N^2 t_f(\delta t)^4$ [1]. With $\delta t = 2^{-10}$, $N = 50$ and $t_f \sim O(10^5)$, $\delta\xi \sim 9x10^{-4}$ giving an error that is less than 0.1% for both node position and velocity. These values give no significant position error and time delay on the onset of fragmentation [1].

By subjecting a two-dimensional lattice to biaxial stretching and looking at the conservation of energy injected in the system, Esleta *et al*. also found numerical stability of the method with respect to lattice size . From their study, the waiting time t_c which indicates the onset of breaking was found to be linear with respect to lattice size N [1]. $t_c \sim N$ and the average force in each node $\langle F_{node} \rangle \sim 4NF_{app}$ which means that the Hamiltonian will have constant increase with larger grid network sizes. This justifies the choice of our parameters as they are shown to still capture the dynamics of larger grid networks while reducing computational complexity (for RK4, computational complexity is proportional to N^2) [1, 2].

S3. DISTRIBUTION OF INFLUENCE

A. Lattice Network

1. Uniform Force Directions

Forces in a system can be directed uniformly such that the vertical and horizontal applied forces exerted by connected nodes have the same directions. This results to a net force directed diagonally in the network as illustrated in Fig. S3. These initial directions of F^k_{app} between neighboring nodes are maintained throughout the simulation.

Here, the node in the topmost left corner labelled as the source node in Fig. S3 (a) is the least influential node and is influenced by all nodes in the network. Such force directions

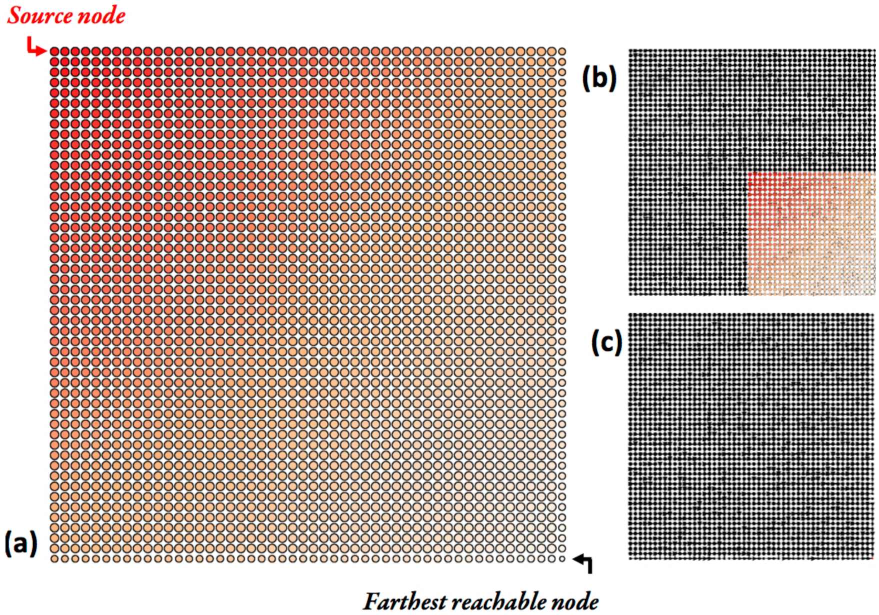

FIG. S3: *Heatmap of a lattice network with uniform force directions.* (a) The node in the topmost left corner is influenced by all other nodes and the degree of influence decreases diagonally towards the farthest reachable node at the bottom right corner. (b) Nodes are influenced only by nodes that are to their right and below them. (c) All forces are directed towards the most influential node in the bottom right corner.

pattern also allows nodes to be influenced only by nodes that are to their right and below them as illustrated in Fig. S3 (b). All forces in the system flow towards the node in the bottom right corner which is the most influential node in the network. This is also the only node which is not influenced by any node in the network.

2. Random Force Directions

The directions of the applied forces in a lattice network are random when the interactions of its components result to random distribution of loading and when the influential nodes of the network are positioned randomly in grid space. We show in Fig. S4 that some nodes are influenced by only a few nodes while others receive much influence. When the force directions are random and not uniform, there are also more agents (6.24%) which are not influenced by any node in the network.

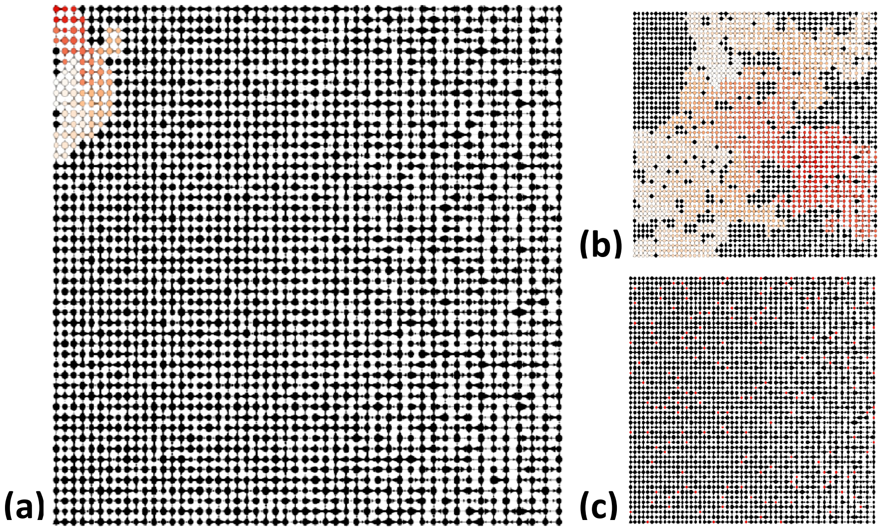

FIG. S4: *Heatmap of a lattice network with random force directions.* Influence is spatially distributed randomly. In (a) only 3.92% of the nodes has influence on the node in the topmost left corner of the network but in (b) we show a node having a greater influence range. (c) There are also more nodes (6.24%) which are not influenced by any node.

B. Erdos-Renyi Network

1. *Uniform Force Directions*

Though connections among nodes in an Erdos-Renyi network are random, force directions can be made as uniform as possible by preferring specific positions in placing influential nodes. In Fig. S5, we see that nodes are influenced only by nodes that are below them. The number of nodes that are not influence by any node accounts for 6.24% of nodes in the network which is similar to the case of lattice networks with random force directions.

2. *Random Force Directions*

In randomizing force directions in an Erdos-Renyi network, we are also distributing the influentials in grid space. For such case, nodes are influenced by other nodes regardless of their position as shown in Fig. S6. There are also more nodes which aren't influenced by any node and this accounts for 14.12% of nodes in the network.

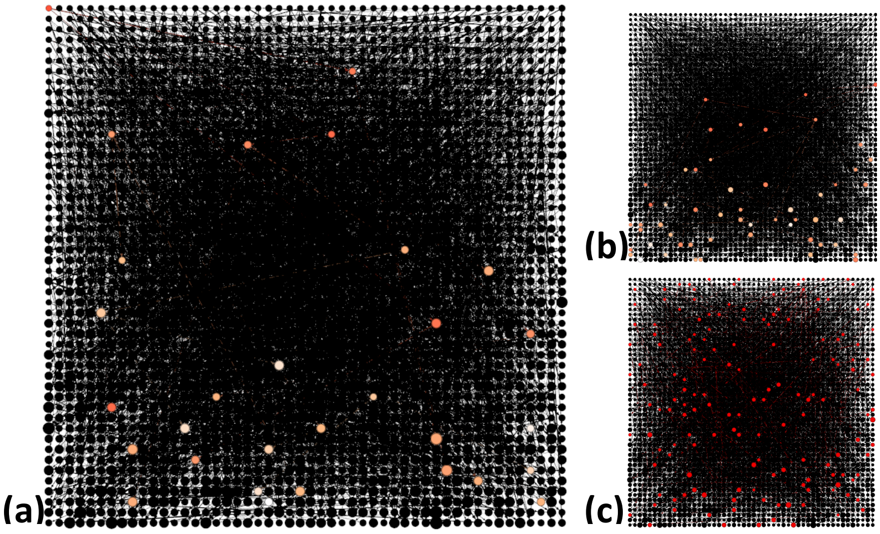

FIG. S5: *Heatmap of an Erdos-Renyi network with uniform force directions.* (a) Nodes can influence nodes that are not their spatial neighbors. The uniformity of force directions is illustrated in (b) where nodes can only be influenced by nodes below them. (c) The number of nodes that are not influenced by any node accounts for 6.24% of nodes in the network.

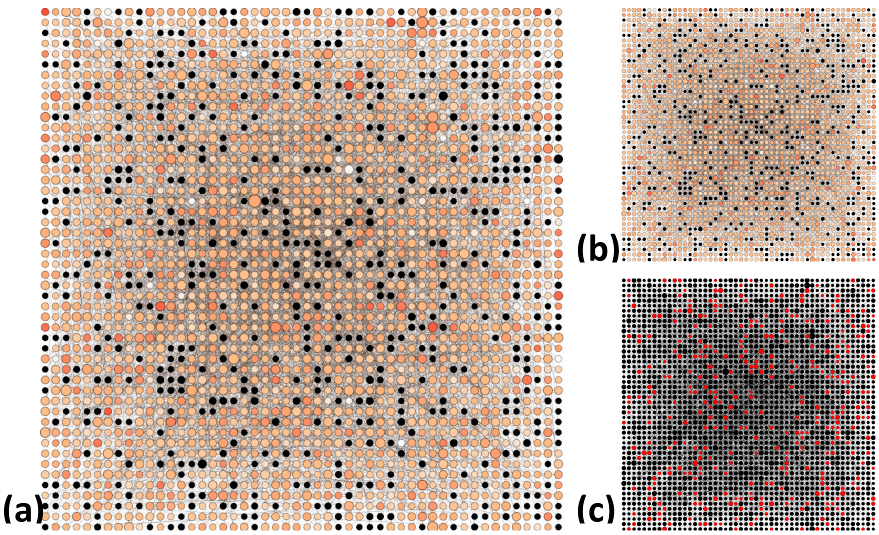

FIG. S6: *Heatmap of an Erdos-Renyi network with random force directions.* (a) Nodes are influenced by more nodes when both connections and force directions pattern are random. (b) This is true regardless of the position of the node in grid space. (c) There are also more nodes that are not influenced by any node which accounts for 14.12% of network nodes.

C. Barabasi-Albert Network

1. *Uniform Force Directions*

Almost all of the edges of the Barabasi-Albert network considered were directed outward and all non-zero node in-degrees are only at most $k_{in} = 2$. Owing to the scale-free degree distribution of the Barabasi-Albert network, the hubs account for almost all of the edges. By restricting all of the edges of the hubs to be directed outward, and all others to prefer a certain direction, uniformity in force directions can be attained as shown in Fig. S7. This resulted to the hubs having a path to almost all nodes while other nodes have very few connections. 49.28% of the nodes has no outgoing edge and hence resulted to most of the nodes having only a few path connections.

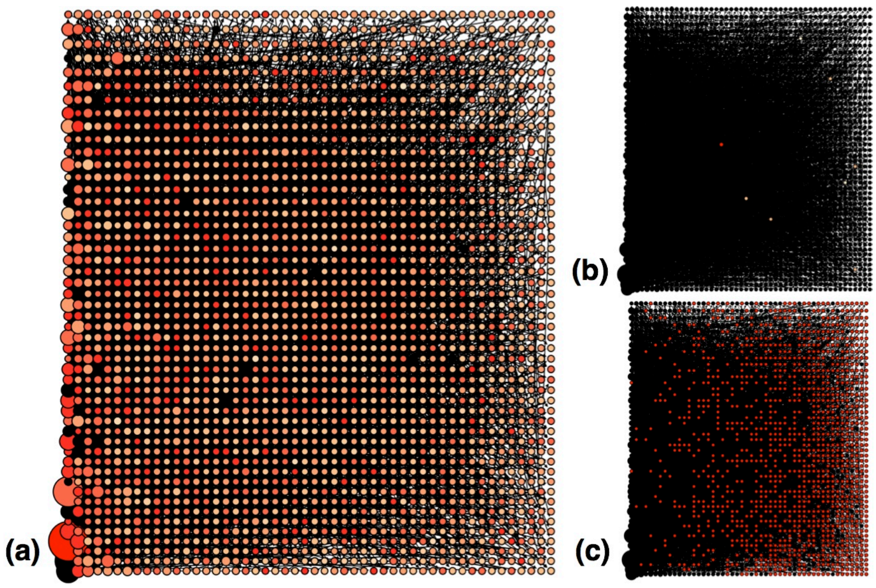

FIG. S7: *Heatmap of a Barabasi-Albert network with uniform force directions.* (a) The node with the highest degree is connected to almost all nodes. As illustrated in (b), due to the uniformity of force directions and the scale-free degree distribution, other nodes are connected to very few nodes. (c) 49.28% of nodes in the network has no outgoing edge.

2. Random Force Directions

For the Barabasi-Albert network with random force directions, the number of edges directed outward is about the same as those directed inward. Randomizing force directions created more paths among the nodes. All nodes regardless of their degree or number of connections have paths to a significant number of nodes in the network as shown in Fig. S8. This lead to less nodes having no outgoing edge (68.26% reduction in nodes with no outgoing edge) which in effect distributes influence in the network.

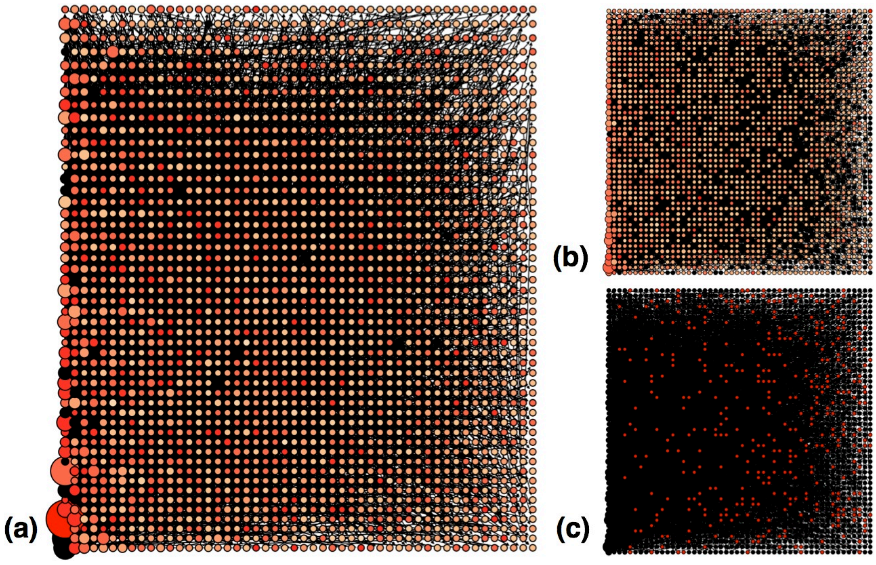

FIG. S8: *Heatmap of a Barabasi-Albert network with random force directions.* (a) The node with the highest degree is connected to almost all nodes. (b) Randomizing force directions allowed other nodes to have paths to more nodes. (c) 15.64% of nodes in the network has no outgoing edge.

S4. BARABASI-ALBERT NETWORK CONFIGURATIONS

The fraction of disconnected edges shown in Fig. 6(e-f) and the lifetime of grid networks of Barabasi-Albert networks in Fig. 8 are averages of two configurations of network hub placement, (1) when the hubs are placed next to each other at the corner of the grid as in Fig. S9(a, c and e) and (2) when the hub placements are shuffled as in Fig. S9(b, d and f). Additionally, for the uniform force directions case, both (a) edges directed away from the

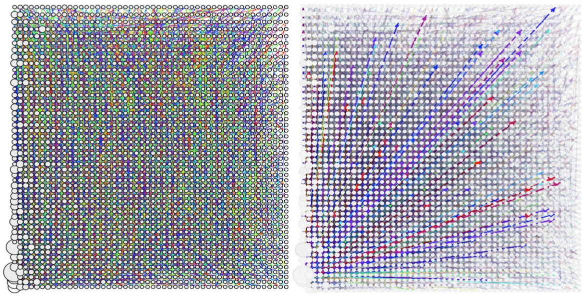

(a) hubs in corner, edges away from higher k node

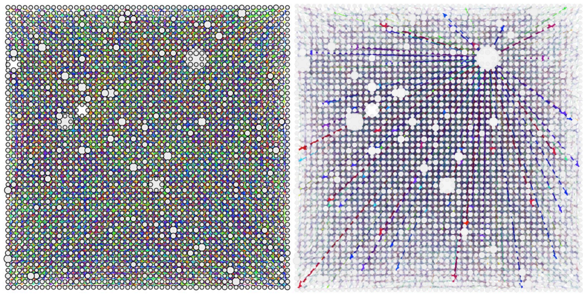

(b) hubs shuffled, edges away from higher k node

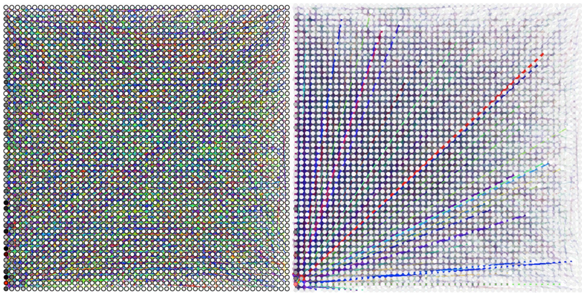

(c) hubs in corner, edges towards higher k node

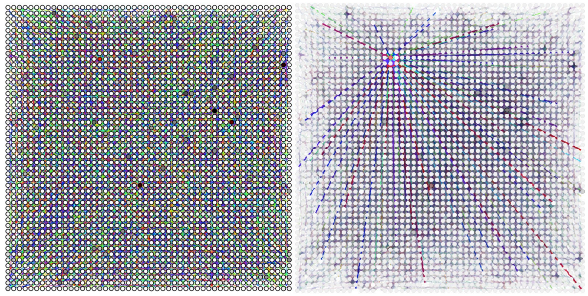

(d) hubs shuffled, edges towards higher k node

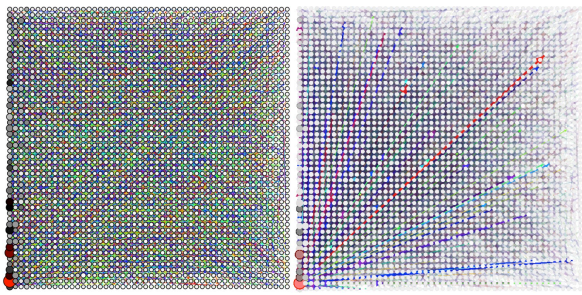

(e) hubs in corner, edges in random directions

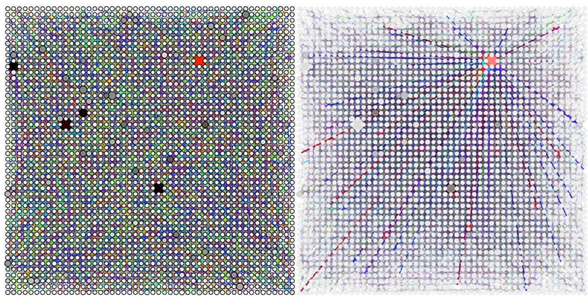

(f) hubs shuffled, edges in random directions

FIG. S9: *Barabasi-Albert network configurations.* Hubs are either placed next to each other at the corner (a,c,e) or in random positions (b,d,f). Edges in both placements are directed away from the node with the higher degree k (a,b), towards the node with the higher degree k (c,d) or randomly (e,f).

node with the higher degree as depicted in Fig. S9(a and b) and (b) edges directed towards the node with the higher degree as shown in Fig. S9(c and d) are included in the results presented.

S5. GENERALIZATION TO OTHER KINDS OF SPATIAL NETWORKS

Starting with an initial spatial grid network with N x M nodes located in all intersections made by the $(N-1)$ x M + $(M-1)$ x N edges, we can obtain other spatial arrangements by finding a spatial grid network with the least number of intersections such that the actual spatial network can be overlapped unto it in such a way that every node corresponds to one and only one intersection in the initial spatial grid network. That is, we look for d given below which represents the d x d size of each cell in our initial spatial grid network.

$$d = min(GCD(\{\Delta x_{i,i+1}\}), GCD(\{\Delta y_{i,i+1}\})) \tag{1}$$

where $i = 0, ..., n-1$, n is the number of nodes, $\{\Delta x_{i,i+1}\}$ is the set of horizontal distances between the i^{th} and $(i+1)^{th}$ node, and $\{\Delta y_{i,i+1}\}$ is the set of vertical distances between the i^{th} and $(i+1)^{th}$ node such that

$$\Delta x_{i,i+1} \% d = 0 \tag{2}$$

$$\Delta y_{i,i+1} \% d = 0. \tag{3}$$

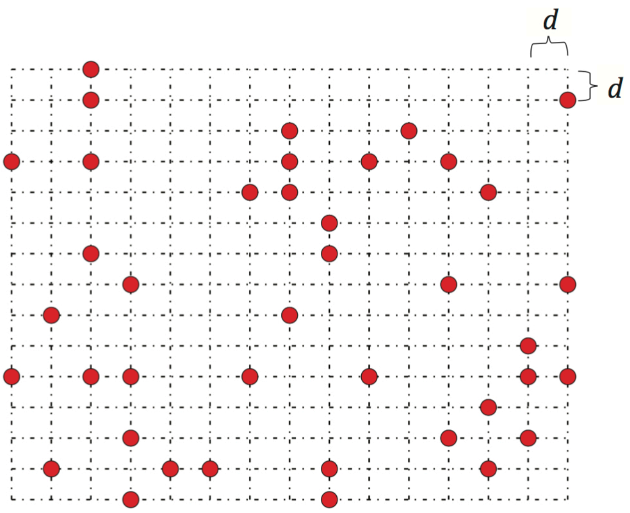

FIG. S10: *Spatial Grid.* For any spatial arrangement of nodes, a smallest spatial grid can be found such that all nodes lie in one and only one intersection in the grid.

We retain the nodes of the initial spatial grid network that corresponds to a node in the actual spatial network and remove those that does not correspond to any node in the actual spatial network. Hence, although most real world networks are not arranged spatially in a

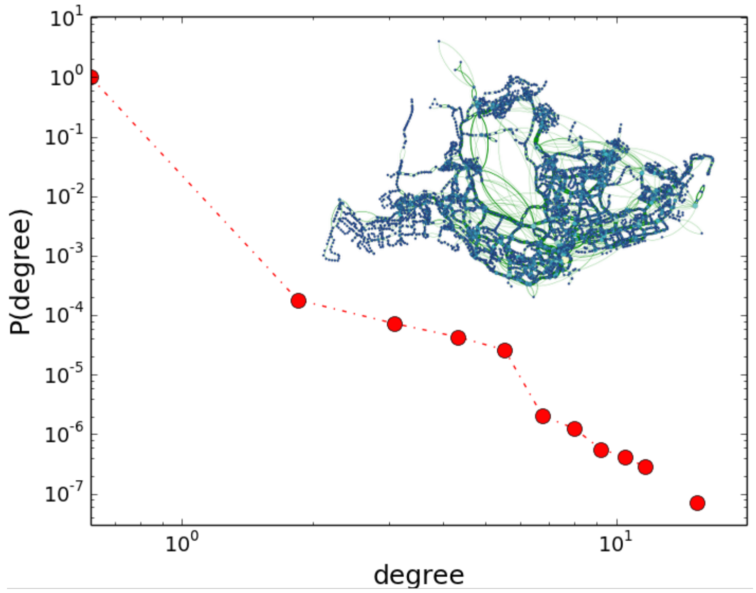

FIG. S11: Degree distribution of Singapore bus network.

grid, we can extend the model developed for spatial grid networks to other networks with a different kind of spatial arrangement by systematically removing nodes to mimic real world networks we want to apply the model to.

S6. APPLICATION TO BUS TRANSPORT NETWORK

The dynamical model of network evolution presented in this work can be used to explore the resilience of a network under different force magnitudes and directions. We illustrate its use using the actual bus network of Singapore. The nodes of the network as shown in the inset of Fig. S11 are the bus stops and an edge is constructed between bus stop a and b if there's at least one bus service that travels from bus stop a to b. We use the method discussed in section S5 and the actual (longitude, latitude) locations of the bus stops to position them in the grid network.

In the absence of additional data, it can be assumed that the demand capacity of the links is constant across the entire bus grid network. Hence, in simulating the evolution of the bus grid network, the elongation thresholds ϵ_{th} are the same for all edges. For the case of the Singapore bus network, it has been shown that the origin-destination (OD) travel demand is a scale-free distribution [4, 5]. Only a few OD pairs are highly utilised while the rest are rarely used [4, 5]. We can think of the travel demand as the applied force experienced by

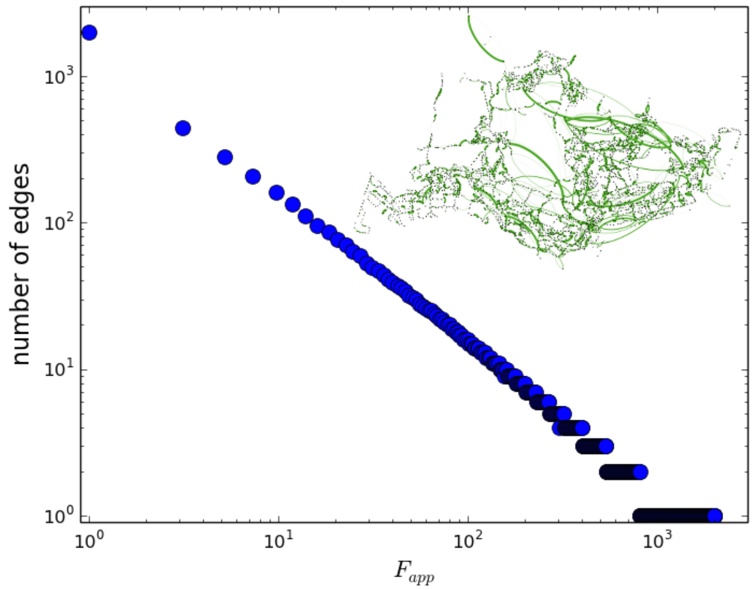

FIG. S12: *Number of edges for each Fapp.* Inset shows bus network edges weighted by F_{app}.

every connected set of nodes. The applied forces can then be made to vary according to

$$number\ of\ edges = 2000\ \times\ (F_{app})^{-1}, \tag{4}$$

which is similar to the relationship between the number of OD pairs and number of journeys per OD pair found in [4, 5]. The assignment of F_{app} according to Eqn. 4 is done by randomly choosing from a biased list of edges with the probabilities of selection proportional to the number of bus routes that includes each OD pair. The OD pair edge used the most has a higher probability of being assigned the largest F_{app}. The number of edges assigned for each F_{app} is shown in Fig. S12.

We vary the directions of the edges to investigate the resilience of the Singapore bus transport network under different bus route directions. The force directions along the edges considered are (a) the actual bus route directions, (b) force directions towards nodes with higher degree, (c) force directions away from nodes with higher degree, and (d) random force directions as shown in Fig. S13.

For the same force magnitudes applied to all edges, the Singapore bus network lasted longest when the force directions were assigned randomly since this method reduces the influence of the higher degree nodes. The next most effective strategy in delaying complete network fragmentation is when forces are directed away from the node, followed by the actual bus directions. Finally the least resilient network is when forces are directed towards

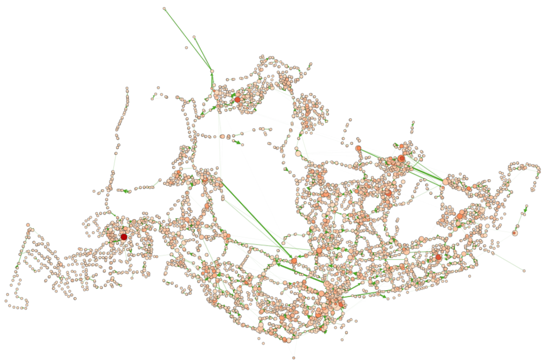

(a) actual bus directions

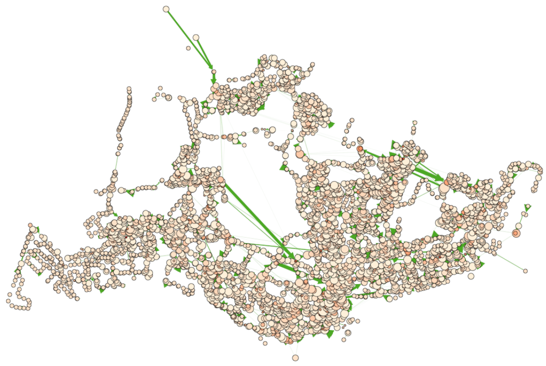

(b) towards higher k node

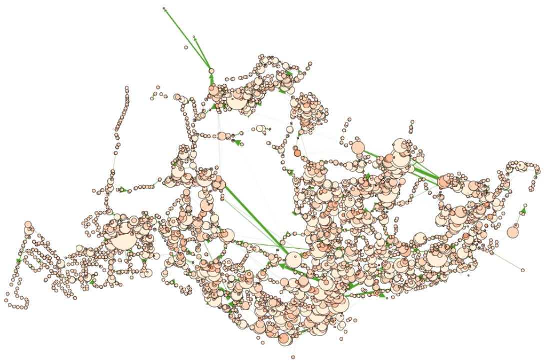

(c) away from higher k node

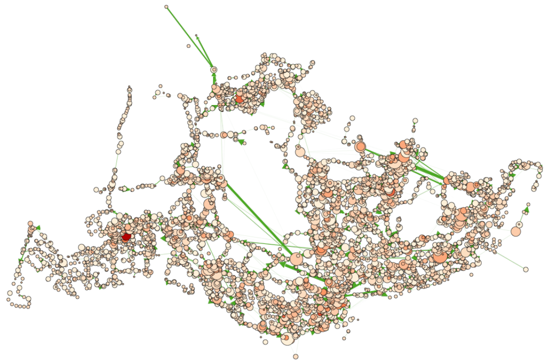

(d) random directions

FIG. S13: *Force directions in Singapore bus network.* Force directions considered are (a) actual bus directions, (b) towards nodes with higher degree k, (c) away from nodes with higher degree k, and (d) random directions. Nodes are colored according to their in-degrees and their sizes are based on their out-degrees. Edges are weighted according to F_{app}.

the higher degree nodes in which case we are increasing the influence of the hubs even more, thereby hastening network collapse.

Using the network lifetime t_f given by the model as a measure of resilience, we can probe the effect of specific changes in bus route directions on the robustness of the transport network. Coupled with travel demand models, this will aid urban planners in constructing a more robust and resilient transport network.

S7. CLUSTER SIZES

To further explore which among the networks considered is the most resilient, we show the fragmentation and evolution of cluster sizes in lattice, Erdos-Renyi, and Barabasi-Albert

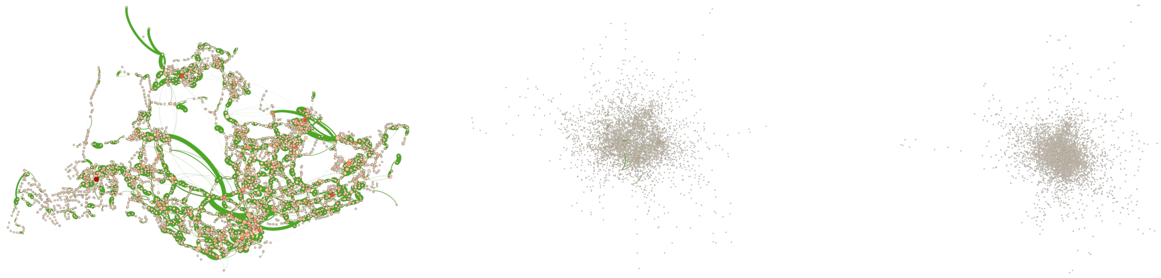

(a) t = 0.0 (b) t = 11.0 (c) t = 31.125

FIG. S14: *Singapore bus network evolution with actual bus routes as force directions.* The network completely fragments at $t = 31.125$. Nodes are colored according to in-degrees and their sizes are based on out-degrees. Edges are weighted according to F_{app}.

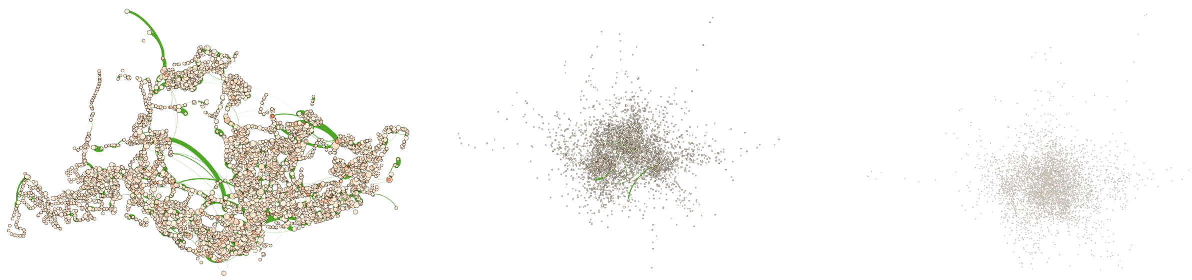

(a) t = 0.0 (b) t = 11.0 (c) t = 26.0625

FIG. S15: *Singapore bus network evolution with forces towards nodes with higher degree.* The network completely fragments at $t = 26.0625$. Nodes are colored according to in-degrees and their sizes are based on out-degrees. Edges are weighted according to F_{app}.

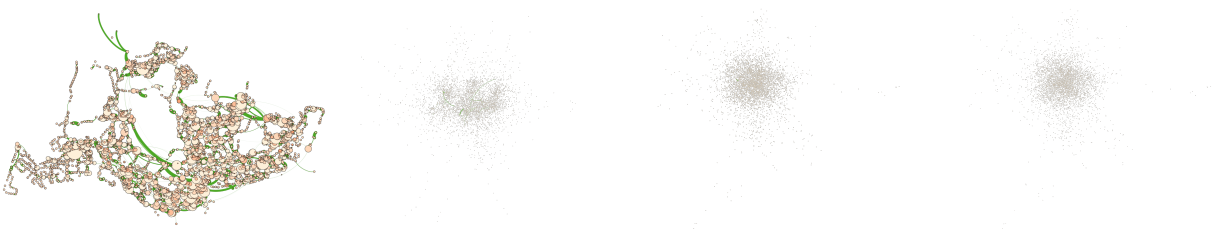

(a) t = 0.0 (b) t = 11.0 (c) t = 32.0 (d) t = 37.4375

FIG. S16: *Singapore bus network evolution with forces away from nodes with higher degree.* The network completely fragments at $t = 37.4375$. Nodes are colored according to in-degrees and their sizes are based on out-degrees. Edges are weighted according to F_{app}.

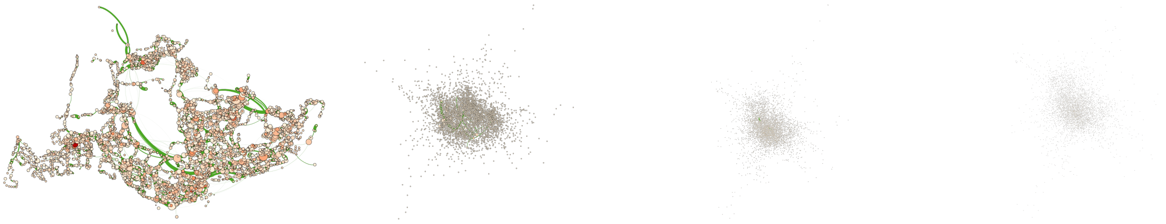

(a) t = 0.0 (b) t = 11.0 (c) t = 32.0 (d) t = 52.75

FIG. S17: *Singapore bus network evolution with random force directions.* The network completely fragments at $t = 52.75$. Nodes are colored according to in-degrees and their sizes are based on out-degrees. Edges are weighted according to F_{app}.

networks for $F_{app} = 0.6$. From Fig. S18, we find that although the lattice network with random force directions starts to break early in the simulation, it eventually becomes the least fragmented.

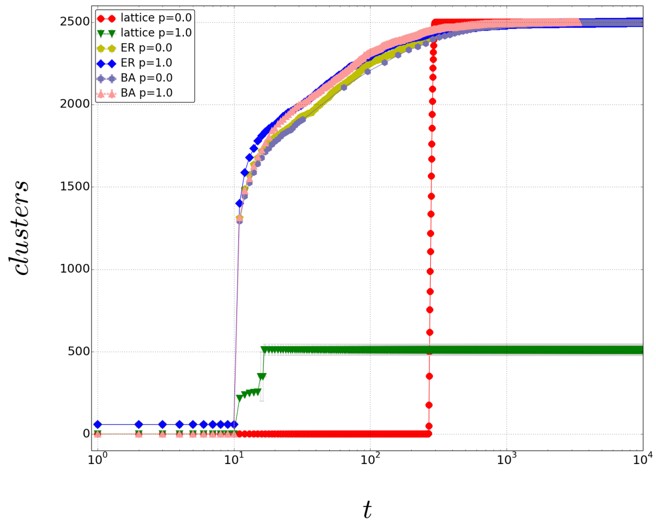

FIG. S18: *Number of clusters in the evolving lattice, Erdos-Renyi (ER) and Barabasi-Albert (BA) networks for* $F_{app} = 0.6$. A lattice with random forcing directions experiences the least amount of fragmentation.

Fig. S19 also shows that when the force sources are positioned randomly in the lattice network, a giant cluster remains intact in the network. However, for the case of positioning the force sources uniformly on the lattice network, the final configuration of the network consists of small clusters with no giant cluster. For small time scales, a lattice network with uniform force directions is more robust. However, longer time scales entail the need to randomize the position of the influential nodes in the lattice network to prevent total network collapse.

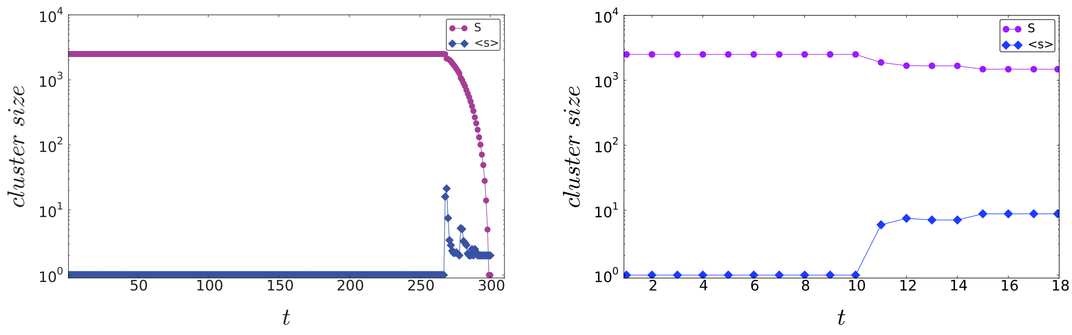

(a) (b)

FIG. S19: *Cluster sizes of lattice networks.* Size of the largest cluster S and the average size of the smaller clusters $< s >$ as the lattice network is subjected to (a) uniform and (b) random force directions with $F_{app} = 0.6$. Random force directions leads to a percolating cluster while uniformity in force directions causes nodes to detach from each other.

The Erdos-Renyi network (Fig. S20), on the other hand, fragments significantly early on in the evolution of the network. But the subsequent fragmentation of its clusters is much slower than in the lattice network. This initial fast rate of fragmentation of the Erdos-Renyi network can be attributed to its initial structure having several clusters as opposed to the lattice network which starts as one giant cluster.

From Fig. S18, the fragmentation of the Barabasi-Albert network resembles that of the Erdos-Renyi network. However, examining the size of the largest component (Fig. S20 and S21) reveals that the presence of hubs in a Barabasi-Albert network slows down further the fragmentation of the largest cluster in the early stages of fast breakings as compared to an Erdos-Renyi network.

---

[1] G. A. Esleta and C. Monterola, Comput. Phys. Commun. **178**, 625-646 (2008).

[2] G. A. Esleta and C. Monterola, Int'l. J. of Modern Phys. C **20**, 1049-1062 (2009).

[3] R. Albert, H. Jeong and A. Barabasi, Nature **406**, 378-382 (2000).

[4] C. Monterola, "Cascade of Travel Duration Delays in a Rapid Transport System". Paper pre-

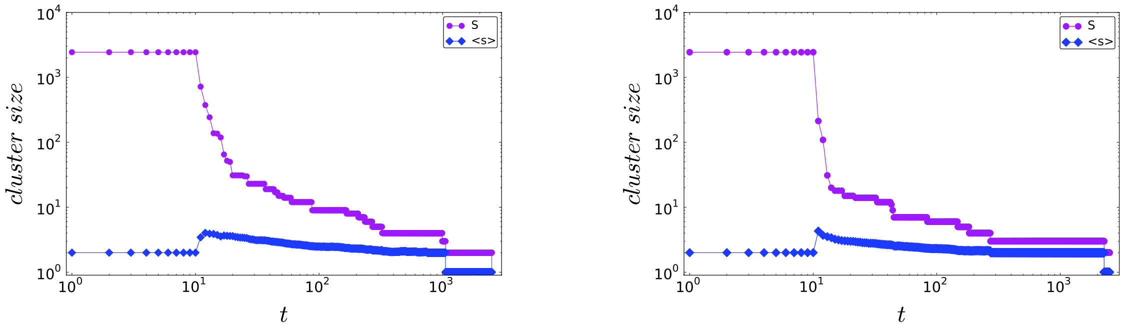

(a) (b)

FIG. S20: *Cluster sizes of Erdos-Renyi networks.* Size of the largest cluster S and the average size of the smaller clusters $< s >$ as the Erdos-Renyi network is subjected to (a) uniform and (b) random force directions with $F_{app} = 0.6$. The network fragments early on in its evolution leading eventually to isolated nodes.

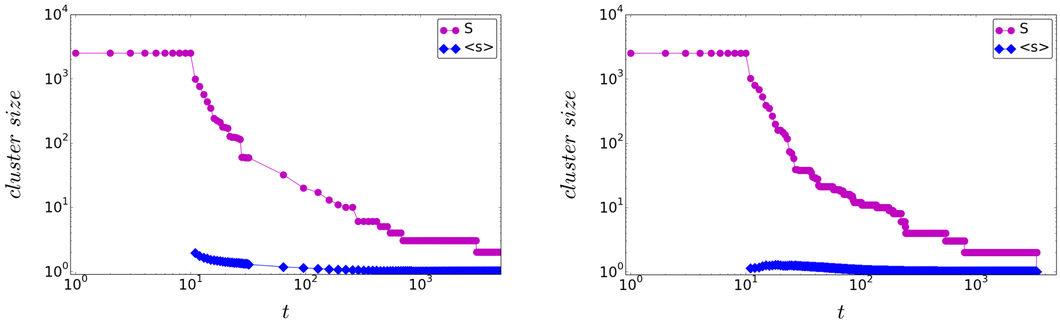

(a) (b)

FIG. S21: *Cluster sizes of Barabasi-Albert networks.* Size of the largest cluster S and the average size of the smaller clusters $< s >$ as the Barabasi-Albert network is subjected to (a) uniform and (b) random force directions with $F_{app} = 0.6$.

sented at European Conference on Complex Systems 2013: Infrastructures, Planning, and Environment, World Trade Center, Barcelona, Spain. (2013, September 17)

[5] E. F. Legara, "Designing Better Transport for a Liveable Singapore". Paper presented at Towards Large Multiscale Simulations of Complex Socio-Economic Systems with Heterogeneous Interacting Agents: Winter Workshop 2013, Nanyang Technological University, Singapore. (2013, November 19)